Supporting information

Atomically ordered intermetallic PdZn coupled with Co Nanoparticles as a highly dispersed dual catalyst chemically bonded to N-doped carbon for boosting oxygen reduction reaction performance

Min Bao[1], Xinghua Chen[1], Shiyu Hu[1], Linqun Zhang[2], Ying Li[1,3,4*], Carlo Carraro[3,4], Roya Maboudian[3,4], Wei Wei[1], Yuanjian Zhang[1], Songqin Liu[1]

[1] Jiangsu Engineering Laboratory of Smart Carbon-Rich Materials and Device, School of Chemistry and Chemical Engineering, Southeast University, Nanjing 211189, China.

[2] Analytical & Testing Center, Nanjing Normal University, Nanjing 210023, China.

[3] Berkeley Sensor & Actuator Center, University of California, Berkeley, California 94720, USA

[4] Department of Chemical and Biomolecular Engineering, University of California, Berkeley, California 94720, USA

*Corresponding Author: Ying Li, Tel: +86-25-52090613; E-mail address: yingli@seu.edu.cn.

Section S1. Supplementary for electrochemical measurements

The Koutecky-Levich (K-L) plots are constructed according to the polarization curves by using rotating ring-disk electrode (RRDE) to analyze the ORR kinetics with the following equation:

$$\frac{1}{J} = \frac{1}{J_{\mathrm{K}}} + \frac{1}{J_{\mathrm{L}}} = \frac{1}{J_{\mathrm{K}}} + \frac{1}{B\omega^{1/2}} \quad (1)$$

$$B = 0.62nFC_0(D_0)^{2/3}\nu^{-1/6} \quad (2)$$

$$J_K = nFkC_0 \quad (3)$$

in which J, J_K, and J_L represent the measured, kinetic, and limiting diffusion current densities, respectively. The kinetic current density (J_K) can be derived from the experimental data detected with rotating disk electrodes at 0.75 V by using the Koutecky-Levich Equation. ω is the electrode rotation rate. n is the transferred electron number of oxygen reduction, F is the Faraday constant (96485 C mol^{-1}), k is the rate constant of the reaction, C_0 is the oxygen-saturated concentration in 0.1 M KOH (1.2×10^{-3} M), D_0 is the oxygen diffusion coefficient (1.9×10^{-5} cm^2 s^{-1}), and υ is the kinetic viscosity of solvent (0.01 cm^2 s^{-1}).

The percentage of H_2O_2 in the product of ORR and the electron transfer number (n) were determined on the basis of the following equations:[1]

$$H_2O_2(\%) = 200 \times \frac{I_R/N_0}{(I_R/N_0) + I_D} \quad (4)$$

$$n = 4 \times \frac{I_D}{(I_R/N_0) + I_D} \quad (5)$$

where I_D is the disk current, I_R is the ring current, and N_0 is the ring collection efficiency of RRDE (0.42) calculated in a solution of 5 mM $K_4Fe(CN)_6$ and 5 mM $K_3Fe(CN)_6$.

To evaluate the polarization, the Tafel equation was constructed based on the following equation:

$$\eta = a + b \times \log|j| \quad (6)$$

where η is the overpotential, a and b are the Tafel constant, and j is the current density.

Section S2. Supporting figures

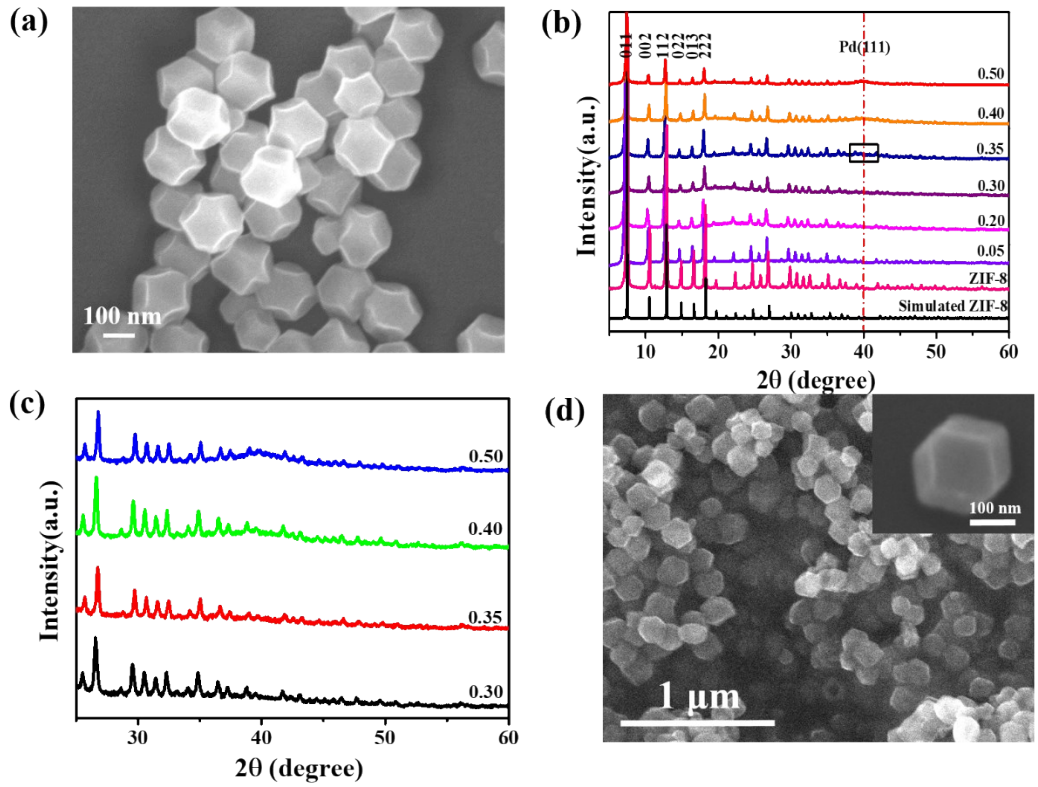

Fig. S1 (a) Field-emission scanning electron microscope (SEM) images of ZIF-8. (b) X-ray diffraction (XRD) patterns of Pd@ZIF-8 with different *r*. (c) The enlarged pattern of (b). (d) SEM image of BiM-ZIF.

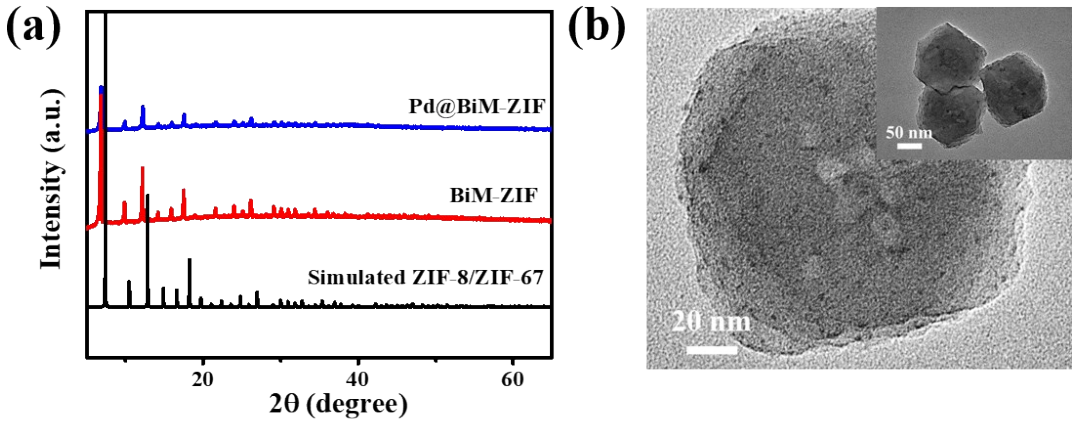

Fig. S2 (a) XRD patterns of simulated ZIF-8/ZIF-67, BiM-ZIF, and Pd@BiM-ZIF. (b) TEM image of Pd@BiM-ZIF.

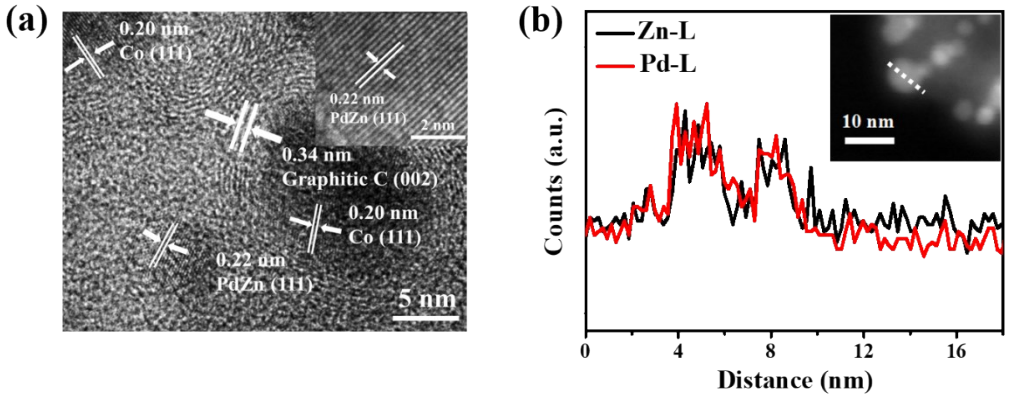

Fig. S3 (a) High-resolution transmission electron microscope (HRTEM) of PdZn/Co/NC. (b) Line scan profile of one ordered PdZn (o-PdZn) nanoparticle taken along the dash line in the inset picture.

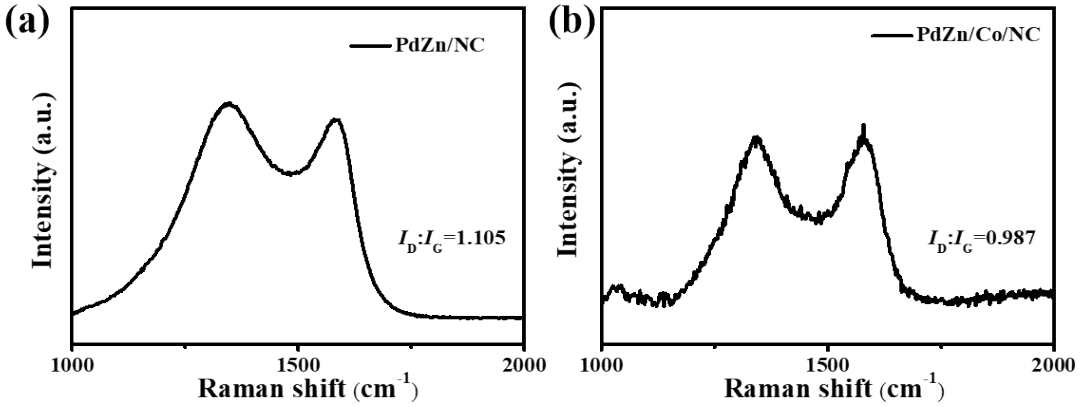

Fig. S4 Raman spectra of (a) PdZn/NC with r = 0.35 prepared at 900 ℃, and (b) PdZn/Co/NC.

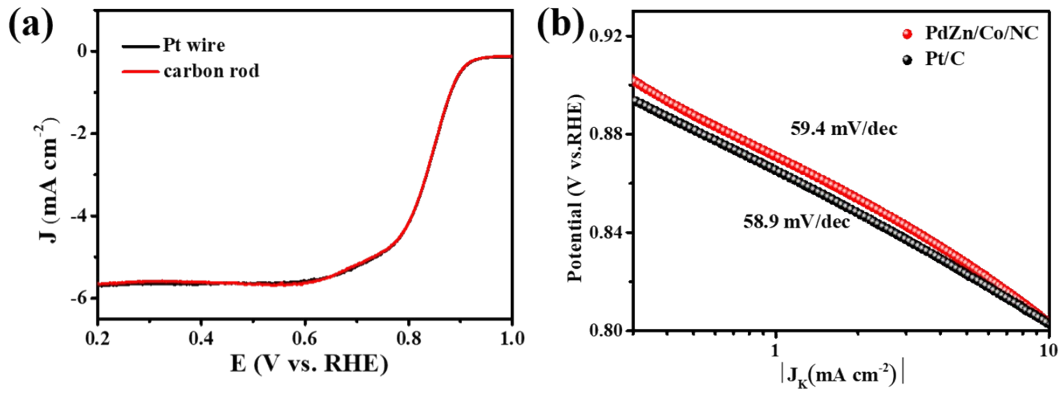

Fig. S5 (a) Polarization curves of PdZn/Co/NC using carbon rod and Pt wire as counter electrode, respectively. (b) Tafel plots of PdZn/Co/NC and Pt/C.

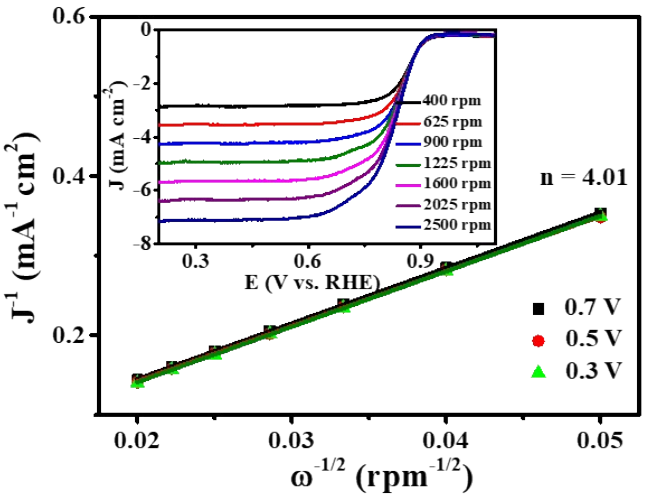

Fig. S6 Koutecky-Levich plots of PdZn/Co/NC at different potentials, inset showing the polarization curves of PdZn/Co/NC at different rotation rates.

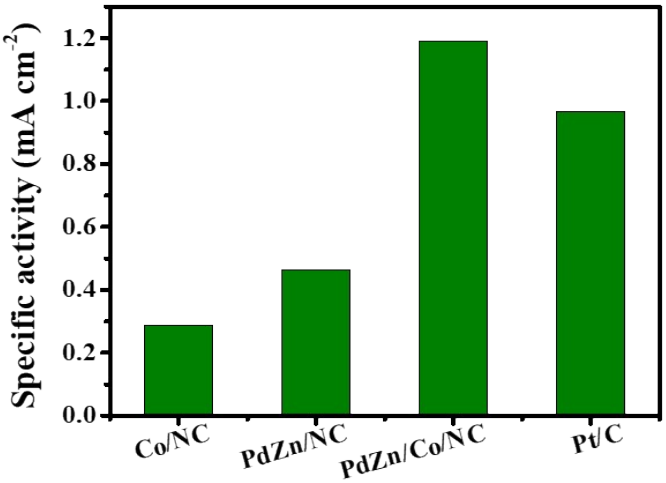

Fig. S7 The kinetic currents of Co/NC, PdZn/NC, PdZn/Co/NC, and Pt/C, normalized based on their corresponding electrochemical surface areas.

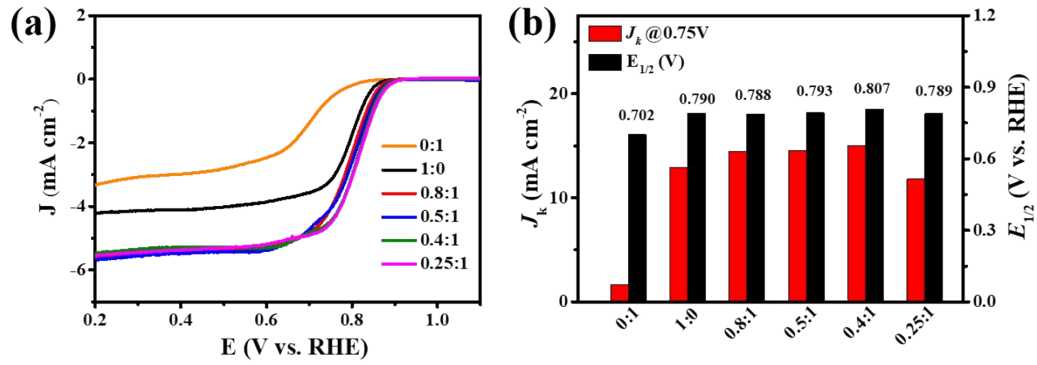

Fig. S8 (a) ORR polarization curves measured at 1600 rpm, (b) J_k at 0.750 V and $E_{1/2}$ of PdZn/Co/NC with different molar ratios of Co and Zn (R). Polarization curves were recorded in O_2-saturated 0.1 M KOH. Scan rate: 10 mV s^{-1}.

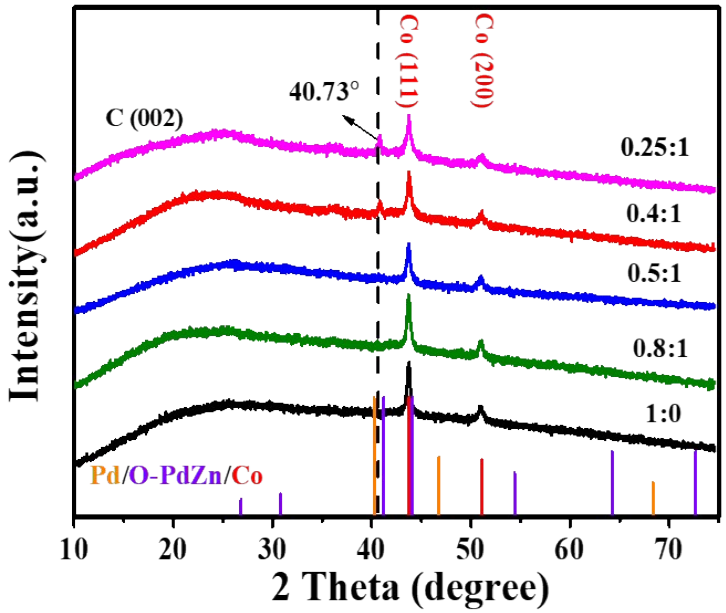

Fig. S9 XRD patterns of PdZn/Co/NC with different molar ratios of Co and Zn (*R*).

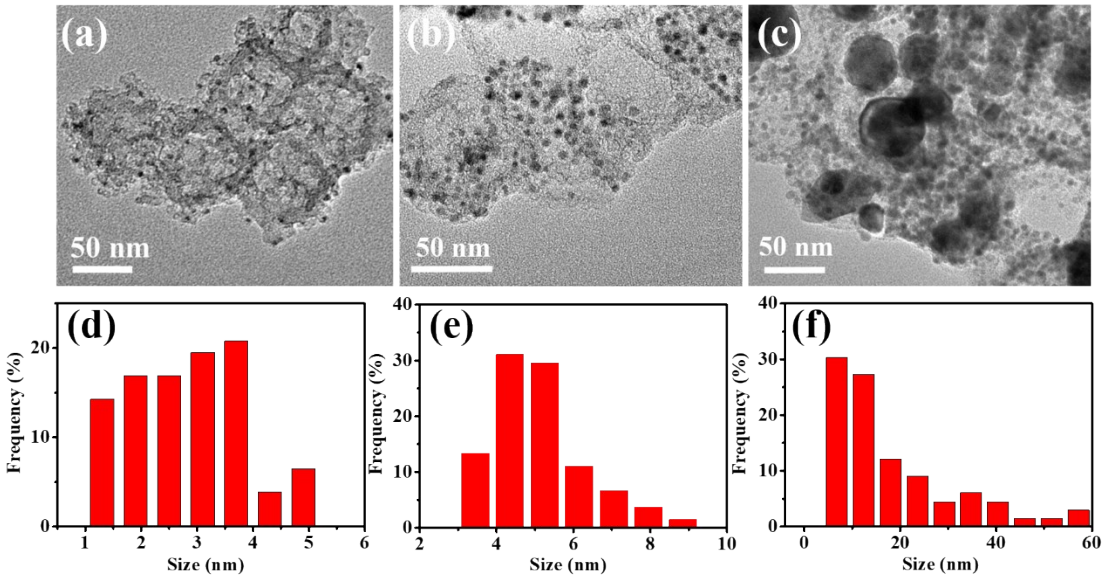

Fig. S10 (a-c) TEM images of PdZn/NC with different molar ratios of Pd and Zn in precursor (r = 0.05, 0.35, and 0.50), and (d-f) corresponding size distributions of metal NPs.

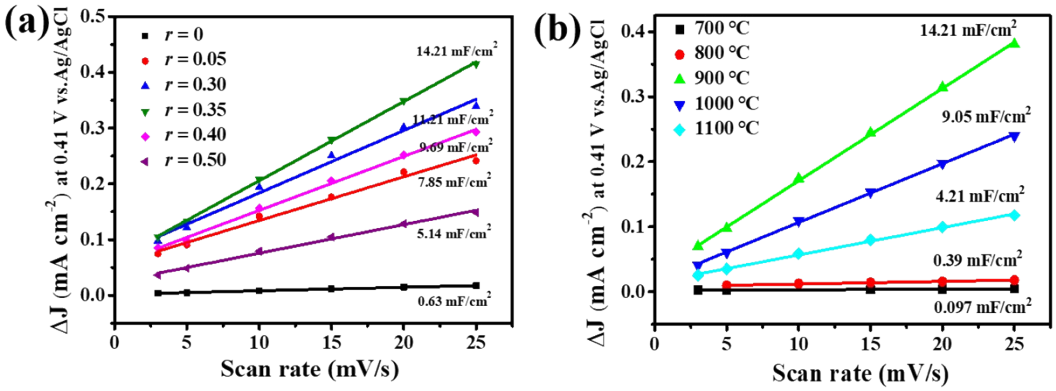

Fig. S11 Dependence of current density differences between positive scan and negative scan as a function of scan rates at 0.41 V for (a) PdZn/NC with different *r*, and (b) obtained at different pyrolysis temperatures. The C_{dl} values indicate that the electrochemical active area reaches the maximum when PdZn/NC with r = 0.35, T = 900 ℃.

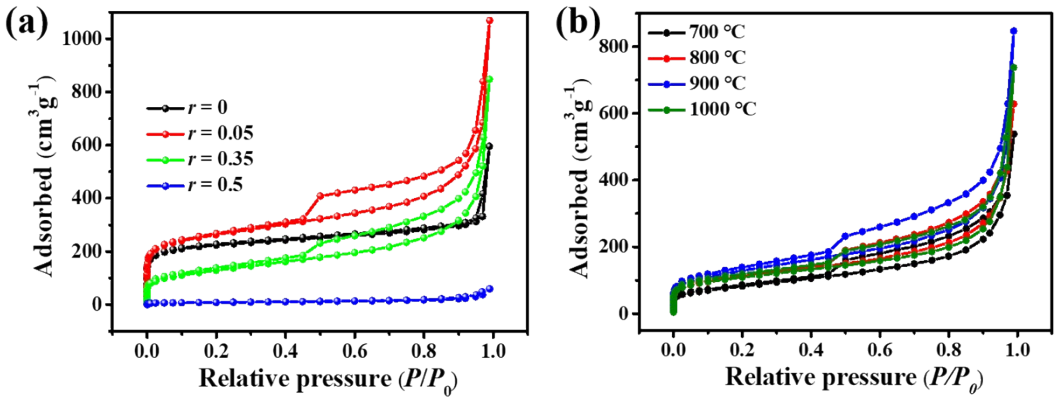

Fig. S12 N_2 adsorption-desorption isotherms of PdZn/NC (a) with different molar ratios of Pd and Zn in precursor (*r*), and (b) obtained at different calcination temperatures (*T*).

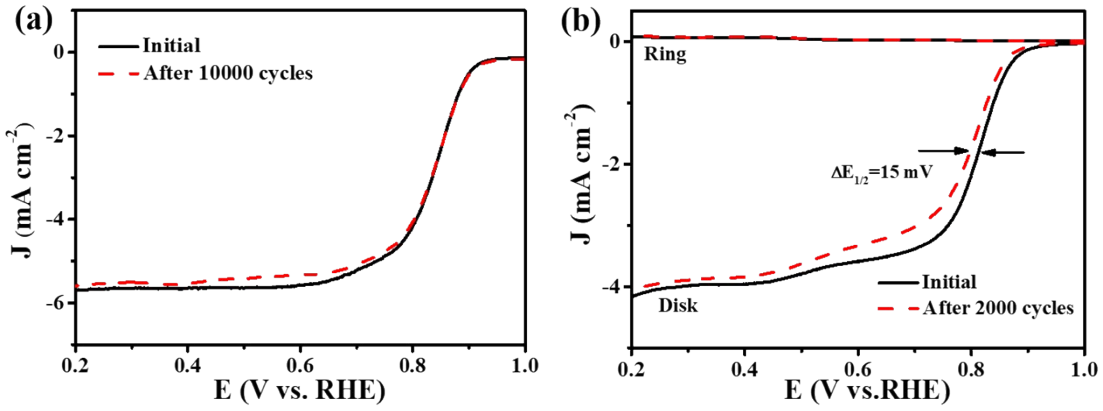

Fig. S13 The ORR polarization curves for (a) o-PdZn/Co dual catalyst, and (b) Pt/C. The dash LSV curves were obtained after cyclic voltammetry (CV) scanning in the potential range between 0.55 and 0.97 V (vs. RHE) for 10000 or 2000 cycles at a scan rate of 250 mV s^{-1} in O_2-saturated 0.1 M KOH by using RRDE.

Section S3. Supporting tables

Table S1 Analysis of N_2 adsorption and desorption isotherms of ZIF-8 and Pd@ZIF-8 with various molar ratios of Pd guest and Zn in host (*r*). Micropore volume and surface are analyzed by t-plot method.

Samples	Micropore Volume (cm^3 g^{-1})	Micropore Surface (m^2 g^{-1})
ZIF-8	0.62 ± 0.02	1664 ± 4
Pd@ZIF-8 (*r* = 0.05)	0.59 ± 0.02	1503 ± 5
Pd@ZIF-8 (*r* = 0.20)	0.57 ± 0.04	1491 ± 4
Pd@ZIF-8 (*r* = 0.30)	0.52 ± 0.02	1322 ± 3

Pd@ZIF-8 (r = 0.35)	0.46 ± 0.03	1278 ± 2
Pd@ZIF-8 (r = 0.40)	0.42 ± 0.03	1080 ± 2
Pd@ZIF-8 (r = 0.50)	0.37 ± 0.02	944 ± 1

Table S2 The ORR activity in 0.1 M KOH for different materials.

Catalyst	E_{onset} (V vs. RHE)	$E_{1/2}$ (V vs. RHE)	J_L (mA cm^{-2})
ZIF-8	0.648	0.478	0.93
Pd@ZIF-8	0.662	0.574	1.35
BiM-ZIF	0.676	0.559	1.25
Pd@BiM-ZIF	0.725	0.634	1.75
Co/NC	0.849	0.765	4.49
PdZn/NC	0.849	0.766	5.30
PdZn/Co/NC	0.916	0.837	5.70
Pt/C	0.910	0.835	5.30

Table S3 Comparison of the ORR activity in 0.1 M KOH for some recently reported Pd-based and Co-based catalysts.

Catalyst	E_{onset} (V *vs.* RHE)	$E_{1/2}$ (V *vs.* RHE)	J_L (mA/cm^2)	n	Refs
PdZn/Co/NC	0.916	0.837	5.70	4.01	This work
Co-N/CNFs	0.820	0.700	5.50	3.88	[2]
Pd@PdO-Co_3O_4	0.923	0.727	5.00	3.90	[3]
Pt@Pd NFs/rGO	0.910	0.820	4.80	3.91	[4]
PdAu alloy	/	0.810	2.20	4	[5]
Pd/TiO_{2-X}:N	/	0.810	5.10	4.02	[6]

$Co@Co_3O_4$/NC-1	/	0.800	/	3.78	[7]
Pd@Zn	/	0.820	/	3.90	[8]

Table S4 Analysis of N_2 adsorption and desorption isotherms of as-prepared materials. The Brunauer-Emmett-Teller (BET) surface area (S_{BET}), macropore and mesopore volume (V_{macro}), and micropore volume (V_{micro}) are calculated by using the BET, Barrett-Joyner-Halenda (BJH), and t-plot methods, respectively.

Catalyst	S_{BET} (m^2 g^{-1})	V_{macro} (cm^3 g^{-1})	V_{micro} (cm^3 g^{-1})
ZIF-8	1818.686	0.486	0.617
Pd@ZIF-8 (r = 0.05)	1623.305	0.528	0.593
Pd@ZIF-8 (r = 0.35)	1401.722	0.637	0.464
Pd@ZIF-8 (r = 0.50)	1126.723	0.539	0.368
PdZn/NC (r, T)			
r = 0, T = 900 °C	800.306	0.638	0.282
r = 0.05, T = 900 °C	953.995	0.832	0.221
r = 0.35, T = 900 °C	455.590	1.264	0.046
r = 0.50, T = 900 °C	29.531	0.091	0.001
r = 0.35, T = 700 °C	293.024	0.818	0.014
r = 0.35, T = 800 °C	386.458	0.928	0.044
r = 0.35, T = 1000 °C	383.974	1.086	0.055

Section S5. References

1. J. T. Zhang, Z. H. Zhao, Z. H. Xia and L. M. Dai, *Nat. Nanotechnol.*, 2015, **10**, 444-452.
2. Q. Cheng, L. Yang, L. Zou, Z. Zou, C. Chen, Z. Hu, H. Yang, *ACS Catal.*, 2017, **7**, 6864-6871.
3. H. C. Li, Y. J. Zhang, X. Hu, W. J. Liu, J. J. Chen and H. Q. Yu, *Adv. Energy Mater.*, 2018, **8**, 1614-6832.
4. A. T. Xie, J. D. Dai, J. Y. Cui, J. H. Lang, M. B. Wei, X. H. Dai, C. X. Li and Y. S. Yan, *ACS Sustain. Chem. Eng.*, 2017, **5**, 11566-11576.

5. Erikson, H., Sarapuu, A., Kozlova, J., Matisen, L., Sammelselg, V., Tammeveski, K., *Electrocatalysis*, 2015, **6**, 77-85.
6. X. Yuan, X. Wang, X. Liu, H. Ge, G. Yin, C. Dong and F. Huang, *ACS Appl. Mater. Interfaces*, 2016, **8**, 27654-27660.
7. A. Aijaz, J. Masa, C. Rösler, W. Xia, P. Weide, A. J. Botz, R. A. Fischer, W. Schuhmann and M. Muhler, *Angew. Chem., Int. Ed.*, 2016, **55**, 4087-4091.
8. H. Yang, K. Wang, Z. Tang, Z. Liu and S. Chen, *J. Catal.*, 2020, **382**, 181-191.